ELSEVIER

Marine Geology 212 (2004) 61–79

MARINE GEOLOGY
INTERNATIONAL JOURNAL OF MARINE GEOLOGY, GEOCHEMISTRY AND GEOPHYSICS

www.elsevier.com/locate/margeo

Swash-zone sediment transport and foreshore evolution: field experiments and mathematical modeling

Magnus Larson[a,*], Susumu Kubota[b], Li Erikson[a]

[a]*Department of Water Resources Engineering, Lund University, Box 118, S-22100 Lund, Sweden*
[b]*Department of Civil Engineering, Nihon University 1-8-14 Kanda-surugadai, Chiyoda-ku, Tokyo 101-8308, Japan*

Received 10 September 2003; received in revised form 14 June 2004; accepted 26 August 2004

Abstract

Data from field experiments carried out in the swash zone on two Pacific beaches in Japan were analyzed to determine net sediment transport rates and the resulting foreshore response. The experiments involved artificial modification of the foreshore slope with a bulldozer, either making the slope steeper or milder, after which a wide range of measurements were performed as the slope evolved back towards its equilibrium value under the action of the incident waves. A sediment transport formula was developed to predict the net transport rate over many swash cycles and compared with the derived transport rates from the surveys of the foreshore. This formula was then combined with the conservation equation for sediment volume to yield a mathematical model for simulating the foreshore evolution under varying waves and water level. Predictions by the model were compared to measurements yielding satisfactory agreement, although the optimum values on the main calibration coefficient displayed some variation between experiments. Further analysis of a limited number of cases indicated that this coefficient may be dependent upon the ratio between the incident wave period and the swash period, which characterizes the interaction between individual waves in the swash zone. A simple analytical solution was also derived for a schematized foreshore shape to estimate the typical time scale of the morphological response.

Keywords: swash zone; hydrodynamics; sediment transport; morphology; foreshore; mathematical modeling; runup; field measurements

1. Introduction

1.1. Background

The swash zone constitutes the area of the beach where the waves run up and down, dissipating or reflecting their remaining energy after traveling towards shore. Propagation of waves up the beach is typically referred to as uprush, whereas the return of the water is denoted as backwash (thus, uprush and backwash together encompass a swash cycle). The morphologically active part of the beach corresponding to the swash zone is often called the foreshore (or beach face), that is, the part of the beach that is shaped by the hydrodynamic forces in the swash. Although

* Corresponding author. Fax: +46 46 222 4435.
E-mail address: magnus.larson@tvrl.lth.se (M. Larson).

0025-3227/$ - see front matter © 2004 Elsevier B.V. All rights reserved.
doi:10.1016/j.margeo.2004.08.004

the swash zone is a very narrow strip, it is of great importance for the sediment exchange between land and sea, which in turn affects both the subaerial and subaqueous evolution of the beach. Morphological processes such as erosion during severe storms, post-storm recovery, seasonal variation in foreshore shape, and evolution of rhythmic features are all intimately related to this exchange.

Hydrodynamic and sediment transport conditions are highly complex in the swash zone involving, for example, rapidly varying flow (in time and space), nonlinear wave transformation, wave–wave interaction, and multiphase flow with possible infiltration and exfiltration effects. Detailed theoretical studies of swash hydrodynamics are difficult to carry out and they have typically focused on conditions that are in general not encountered on natural beaches (i.e., plane impermeable slopes subject to monochromatic waves). On the other hand, empirical investigations based on field measurements are also difficult to execute in such a manner that the governing processes are satisfactorily understood and quantified (conditions are rapidly changing including strong turbulence; full exposure of the bed to the air during extended periods occur; and bed levels are highly varying with bottom conditions that are hard to define).

In spite of these difficulties, significant progress has been made in the last decade concerning the hydrodynamics and sediment transport conditions in the swash zone and the associated response of the foreshore (Elfrink and Baldock, 2002). Particularly in the last few years several comprehensive field studies have been performed that added insight regarding the physics governing sediment transport in the swash zone. However, few field investigations have simultaneously focused on the sediment transport and the resulting foreshore response. Measurements have often been performed at foreshores in more or less equilibrium, where the transport rate in the uprush is very close to the rate in the backwash, leading to little change in the profile shape during the period of observation. Although such conditions can yield information on the detailed physics of sediment transport at the time scale of individual swash waves, it provides less understanding of the net transport over longer time periods causing significant changes in the foreshore shape.

The limited number of studies available on net transport in the swash and associated changes in the foreshore shape over many wave periods has in turn made it difficult to formulate mathematical models based on an understanding of the governing physics. Previous modeling efforts in relation to beach profile change, for example, have employed geometrical considerations to estimate the sediment exchange in the swash zone (e.g., Kriebel and Dean, 1985; Larson and Kraus, 1989), or ignored this zone altogether by defining the shoreward limit to be in the surf zone (Roelvink and Brøker, 1993). Other, more detailed models, have employed complex wave transformation computations and sediment transport formulas, but failed to validate them towards comprehensive data obtained under realistic conditions (in the laboratory or the field).

1.2. Objectives and procedure

The main objective of this study was to investigate swash-zone sediment transport and foreshore evolution based on some unique field data collected on two Japanese beaches during several experiments. A second aim was to develop a simple mathematical model to calculate the net transport rate on the foreshore representative of many swash cycles that together with the sediment volume conservation equation can describe the evolution of the foreshore under varying incident waves and water levels. As pointed above, only a limited number of previous studies have been concerned with net transport and associated foreshore evolution over many swash cycles where significant changes in the foreshore profile were observed.

The field experiments were carried out between 1990 and 1997 at two Pacific Ocean beaches in Japan. In total six experiments were performed mainly focusing on erosional conditions, although one experiment involved onshore net transport and accretion. In order to induce significant net transport the natural beach slope, which was in equilibrium with the incident waves prior to the experiment, was artificially modified with a bulldozer, leading to a steeper or flatter foreshore profile. A wide range of measurements were then performed on the modified foreshore as the sediment transport induced by the waves made the profile return to its equilibrium shape. By making the foreshore slope deviate significantly from equili-

brium, marked sediment transport and profile change were observed clarifying the relationship between the forcing and the foreshore response.

In the following, a brief literature review is first presented on sediment transport in the swash zone and resulting foreshore response, focusing on previous field experiments. The present field experiments are described, including the study sites, the setup, and the general procedure used. Some measurement results are briefly discussed and the experimental runs are summarized. A sediment transport formula is developed that aims at predicting net transport rates over many swash cycles and this formula is compared to transport rates at the seaward end of the swash zone determined from the measurements. An analytical formulation is derived to quantify the time scale of the foreshore response to estimate how quickly equilibrium will be obtained after a change in the incident wave conditions. In order to further validate the sediment transport formula with respect to the spatial variation across the swash zone, a numerical model is developed where the formula is combined with the sediment volume conservation equation to compute the foreshore evolution. The paper ends with some conclusions and speculations concerning the possible dependence of the main transport coefficient on various physical quantities.

2. Previous work on swash sediment transport and foreshore response

Waddell (1973a,b) carried out a pioneering investigation on the conditions in the swash on a natural beach. The measurement system developed in this study, consisting of capacitance gages placed across the foreshore and connected to a computer for simultaneous sampling, could be used for measuring both the instantaneous water and sand surface levels. It was later copied by several other researchers in their investigations of the swash zone (e.g., Sonu et al., 1974; Hughes, 1992; Kriebel, 1994). Waddell observed that during the uprush, as well as the initial part of the backwash, the leading edge behaved similarly to a unit mass moving up the foreshore slope under the action of gravity, neglecting friction (Shen and Meyer, 1963). However, the initial momentum needed to drive the movement of the swash waves up the slope was larger than expected (compare Miller, 1968). Two water depth maxima were observed during a swash cycle, and the swash frequency was shown to be a function of bore height based on the measurement and some simple theoretical considerations. Waddell (1973a) analyzed the temporal variation in recorded sand surface levels on the foreshore and found evidence of material predominantly moving upslope as suspended load and downslope as bed load.

Richmond and Sallenger (1984a) monitored foreshore sediment level and sediment size during the DUCK82 experiment. Computations of the cross-shore sediment transport based on measured velocities were employed to interpret observed changes in the beach texture. Sallenger and Richmond (1984b) investigated the oscillation in sand levels on the foreshore based on field measurements. The change in elevation at 11 sticks placed on the foreshore was monitored and analyzed. Horn and Mason (1994) studied the transport mode in the swash zone by carrying out field measurements with sediment traps on four different beaches in the UK. Bed load was found to be more important than suspended load, especially for the backwash phase.

Kubota et al. (1994) artificially steepened the foreshore on a natural beach and measured the change in foreshore topography at high resolution in time and space as the beach returned to its equilibrium slope. The original, equilibrium slope was 1/20 and the initial foreshore slope after being steepened was 1/10. Kubota et al. (1997) reported results from four experiments involving artificial modification of the foreshore slope, including making the slope both steeper and milder. Net transport rates derived from the sediment volume conservation equation were compared with the formula proposed by Sunamura (1984). Kubota et al. (1999) determined sediment transport in the swash zone using two different methods: integrating the sediment volume conservation equation (based on change in foreshore topography) and employing streamer-type sand traps. Data from six different field experiments were used where the foreshore was artificially modified to induce transport. An empirically based sediment transport formula for the swash zone was derived based on a wave parameter and the deviation of the slope from its equilibrium value. The field experiments presented by Kubota et al. (1994, 1997, 1993) were utilized in this study.

Hughes et al. (1997a) measured flow velocity and total sediment load in the swash on a steep beach. Maximum velocity was recorded during the passage of the leading edge (uprush), whereas during the backwash the maximum velocity appeared towards the end of the swash cycle. The duration of the backwash was longer than the uprush, as observed by Waddell (1973a). Total load transport measured with sediment traps showed strong correlation with the time-averaged velocity cubed. Hughes et al. (1997b) calculated the sediment transport separately in the uprush and the backwash. Employing a transport formula based on the velocity cubed, different coefficient values were needed for the uprush and backwash phases, as well as for the different beaches studied (transport larger in the uprush). Masselink and Hughes (1998) also measured swash flow velocity and sediment transport on a natural beach and observed the same strong correlation between sediment load and velocity cubed. A Bagnold-type formula was developed with different coefficient values for the uprush and the backwash.

Butt and Russell (1999) recorded the suspended sediment concentration at three vertical levels and the velocity at one level in a field swash zone. The time-averaged cross-shore suspended sediment flux was calculated showing a tendency towards offshore transport during high-energy conditions, especially in the lower part of the water column. Puleo et al. (2000) studied swash-zone sediment transport in the field and measured suspended sediment concentration, surface elevation, and velocity at three cross-shore locations. Suspension was high near the leading edge of the uprush and almost uniform; however, it settled quickly behind the edge. The conditions for the backwash were different from the uprush. Bore-generated turbulence significantly influenced local sediment suspension (see also Longo et al., 2002). Katori et al. (2001) employed a vertical array of streamer traps to measure the on–offshore transport rate in the swash zone on a natural beach. The results indicated that the transport was concentrated in the bottom layer, decreasing at a high rate above the bed.

Holland and Puleo (2001) (see also Holland et al., 1998) measured the swash motion and associated profile change on the foreshore using video technique. The measurements were carried out at the US Army Field Research Facility in Duck, NC, and included the response of the foreshore during the onset of a storm with erosion corresponding to almost 1 m vertical change. Swash edge excursion was well described by a ballistic model including friction, although significant deviations were observed for individual swash events. Changes in the foreshore were related to the difference between the actual swash duration and its value at equilibrium. The swash duration was characterized by the foreshore slope, implying that the rate of change was a function of the deviation of the foreshore slope from the equilibrium value.

3. Field experiments

3.1. Field site and experimental setup

The data on swash-zone sediment transport and foreshore evolution employed in this study were collected during a range of field experiments conducted between 1990 and 1997 at Hasaki Beach and Hiratsuka Beach (Kubota et al., 1994, 1997, 1999). Hasaki Beach is located about 100 km east of Tokyo and Hiratsuka Beach about 60 km south of Tokyo, and both beaches are facing the Pacific Ocean (see Fig. 1). Out of total six field experiments, five were conducted

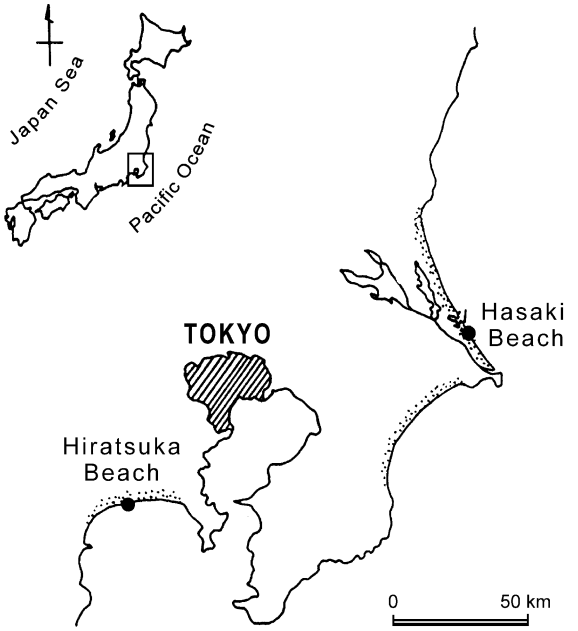

Fig. 1. Location map showing the two sites for the field experiments.

Fig. 2. Artificial mound constructed on the foreshore at Hasaki Beach, Japan, to study swash-zone sediment transport and profile evolution during the experiments carried out in 1995.

at Hasaki Beach and the emphasis of the analysis in this study was on these data. The experiment carried out at Hiratsuka Beach is of interest primarily since it encompassed accretionary conditions, whereas all experiments at Hasaki Beach were for erosional conditions.

An approximately 400-m-long research pier belonging to the Port and Airport Research Institute is located at Hasaki Beach for the purpose of carrying out field studies in the nearshore zone. This pier is equipped with different types of instruments, including six ultrasonic wave gages, and the pier also functioned

Fig. 3. Artificial mound constructed on the foreshore at Hasaki Beach, Japan, to study swash-zone sediment transport and profile evolution during the experiments carried out in 1997.

as a platform for cameras during the experiments to record the wave conditions in the surf and swash zone (e.g., Hotta and Mizuguchi, 1980). The foreshore of the beach is relatively gentle and it is composed of fine sand with a median grain size of about 0.18 mm. At Hiratsuka Beach, the foreshore consists of coarse sand with a median diameter varying between 0.9 and 2.0 mm. The tidal range at both beaches is similar with a typical value of about 1.5 m.

All the experiments were carried out in the same manner: the foreshore slope was first artificially modified during low tide, either steepened or made milder, after which the evolution of the foreshore profile was recorded as it went back to its equilibrium state during rising tide. The reason for modifying the foreshore in this manner was to be able to observe significant net swash-zone sediment transport and profile change. Under natural conditions the foreshore slope would be close to its equilibrium value and only small net transport and changes occur. However, in all experiments but one (1994), measurements were also carried out on the natural beach slope before any artificial modifications, yielding close to zero net transport in the measurements.

Most of the experiments encompassed steepening of the foreshore, in total five experiments carried out in 1992, 1994, 1995, 1996, and 1997 (all at Hasaki Beach), and only one experiment made in 1990 involved reducing the foreshore slope (at Hiratsuka Beach). The modification of the foreshore was made with a bulldozer and a shovel car typically extending about 30 m in the longshore direction and 20 m in the cross-shore direction (depending on the amount of steepening). Mound design (in the case of steepening) was made to include the largest runup heights expected and the sides were stabilized with sandbags to minimize boundary effects. Figs. 2 and 3 illustrate typical mounds constructed on the foreshore at Hasaki Beach during the experiments made in 1995 and 1997, respectively. The sandbags prevented any longshore current on the beach from affecting the swash sediment transport in the area of measurement.

Fig. 4. Measurement setup to record hydrodynamics and sediment transport in the swash zone as well as the foreshore evolution (the research pier at Hasaki Beach visible on the top left side).

Thus, the validity of the present measurements is limited to the situation when the waves are more or less normally incident to the shoreline and no longshore current is generated in the swash. In all experiments, the waves were approximately normally incident close to shore and the measured longshore current was less than 0.2 m/s in the area immediately seaward of the swash zone.

An array of sticks were placed on the modified foreshore normal to the shoreline to measure the profile change, with the sticks placed at an interval of 0.5 or 1 m (see Fig. 4). Video cameras were employed to record the changes in the sand surface level at the sticks. The vertical sticks consisted of 12-mm iron bars to which a measuring tape graded in mm was attached for accurately determining the level. In the final experiment, the level of the beach was recorded at each stick through a wooden bar placed at the bottom end of the stick, ensuring a minimum of scour around the stick. The beach level was recorded every minute during an experiment, which typically lasted for about 2 h. Other measurements simultaneously carried out with the beach level recordings involved sediment transport rates using streamer traps, swash hydrodynamics using a step-type swash gage, and surf-zone waves (seaward of the swash zone) using video cameras, pressure wave gages (PWG), and two-component electromagnetic current meters (EMCM) (not all these types of measurements were carried out during all experiments; see Kubota et al., 1997, 1999;

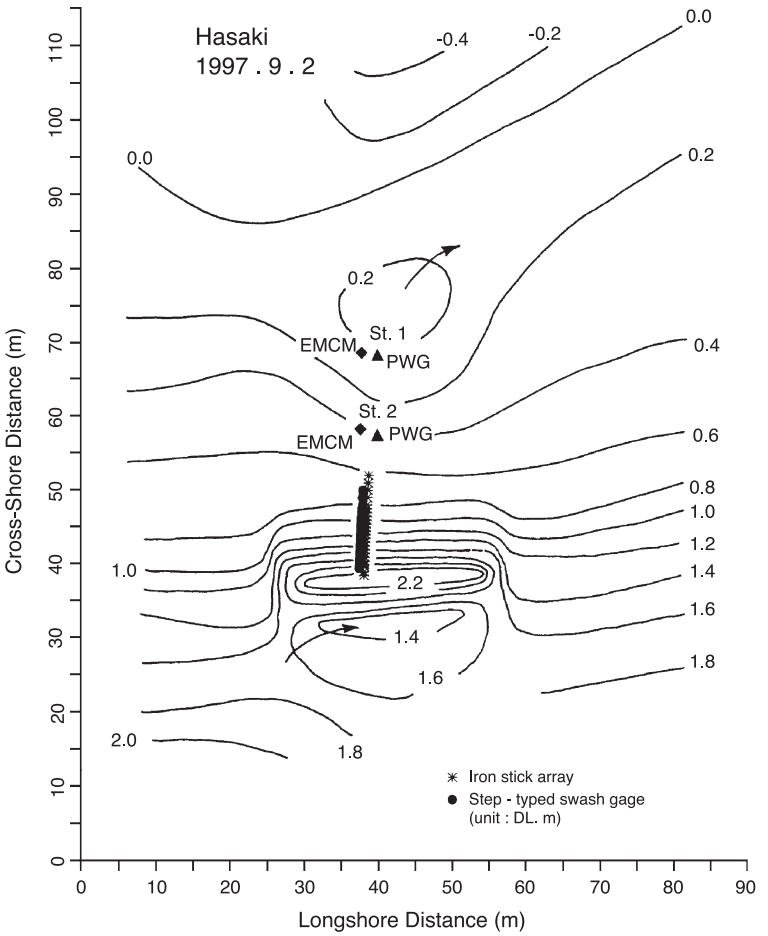

Fig. 5. Beach topography and plan view of instrument arrangement during the 1997 experiment (elevations given with respect to an arbitrary datum line).

for details). Data sampling was made at 5 Hz for the electronic instruments.

Fig. 5 displays a plan view of the typical experimental setup and Fig. 6 the corresponding cross-section (the 1997 experiment). The PWG and EMCM were located at two poles just seaward of the swash zone in water depths between 0.5 and 1.0 m, depending on the tidal elevation. Video cameras were also directed towards these target poles for detailed wave recording. A topographic survey was carried out prior to each experiment, as shown in Fig. 5 (the elevations refer to a datum line, DL, which was locally defined). The location of the PWGs and EMCMs are also shown in this figure together with the stick array and the swash gage (24 sticks were used in the experimental setup displayed in Figs. 5 and 6). Measurements made by the swash gage, encompassing 20 capacitance sensors installed parallel to the stick array, were not used in the present study. Kubota et al. (1999) found a marked correlation between the power in the swash oscillation, determined from the swash gage recording, and the cross-shore current velocity power measured seaward of the foreshore.

Simultaneously with the measurements of profile change on the foreshore, the sediment transport rate was recorded using a streamer-type sand trap. The trap consisted of an entrance part made of metal, a plankton net (mesh size 148 μm), and a bottom plate to reduce the effect of local scour. By employing one trap with the opening in the seaward direction and one in the shoreward direction, the onshore and offshore transport rates could be measured, respectively.

3.2. Experimental runs and measurement results

Table 1 summarizes the runs made during the six experiments, where the notation for a specific run is HA for Hasaki Beach, HI for Hiratsuka Beach, and a two-digit number for the year of the experiment. The letter N at the end denotes a measurement during natural conditions, before any modifications of the foreshore was made. The table also includes the significant wave height and wave period measured at the shoreward end of the surf zone in water depths typically between 0.5 and 1.0 m, depending on the tide and the placement of the gage. Water levels were determined either by video cameras or capacitance wave gages. The net transport rate during each run at the seaward end of the swash zone, determined from integrating the sediment volume conservation equation, is also given. Table 2 presents the dimensions of the mounds constructed on the foreshore during the experiments and the number of

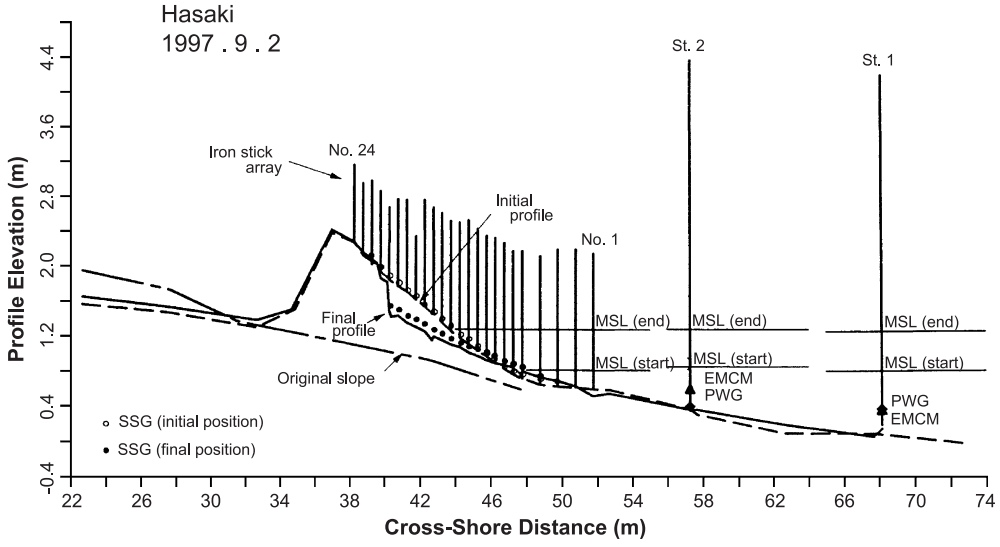

Fig. 6. Initial and final beach profiles and cross-sectional view of instrument arrangement during the 1997 experiment (elevations given with respect to an arbitrary datum line).

Table 1
Overview of runs carried out during the experiments on swash-zone sediment transport and foreshore profile evolution

Run number	Initial slope	Equilibrium slope	Significant wave height (m)	Significant wave period (s)	Net transport rate 10^{-4} (m^3/m/s)
HA97N	0.050	0.050	0.53	7.5	−0.08
HA97-1	0.172	0.050	0.53	12.7	1.00
HA97-2	0.212	0.050	0.68	13.0	2.27
HA96N	0.035	0.035	0.64	10.5	−0.07
HA96	0.100	0.035	0.52	14.1	2.01
HA95N	0.052	0.052	0.68	8.7	0.39
HA95-1	0.090	0.052	0.61	8.0	0.46
HA95-2	0.113	0.052	0.58	8.5	1.32
HA94	0.144	0.050	0.66	11.0	5.30
HA92N	0.057	0.057	0.47	13.4	0.00
HA92	0.097	0.057	0.40	13.5	1.07
HI90N	0.125	0.125	–	–	–
HI90	0.100	0.125	1.27	8.9	−0.67

surveys taken, where a survey was made every minute.

The net transport rate determined from the topography change (i.e., integrating the sediment volume conservation equation) was computed to yield averages on a minute basis. Measured net rates with the sand traps, obtained as the difference between the onshore and offshore rates, were compared with the calculated net rates. However, before comparing with the measurements from the sediment traps, a moving filter was employed to the computed rates to obtain a smoother time variation and reduce occasional local peaks in the transport rate (Kubota et al., 1999). The agreement between the measured and the computed rates was good, which provided additional confidence in the derived transport rate subsequently used for model development and validation.

As an example of the measurement results from an experimental run, Fig. 7 shows recorded profiles during Run HA94 (in total 60 surveys, obtained every minute). This run was somewhat different from the other runs with respect to the shape of initial profile: the artificially steepened foreshore was backed by a small dune-type feature. However, the same basic pattern in the response as for the other runs was observed. The initial foreshore slope was out of equilibrium with the waves and seaward net transport occurred that gradually brought the slope back to its equilibrium value. At the dune, a marked scarp evolved, and the dune face retreated through a cycle of slope increase and collapse resembling an avalanche process. The erosion from the dune increased the seaward transport compared to the other runs, as discussed later in the paper.

Table 2
Horizontal dimensions of the mounds constructed on the foreshore during the swash-zone experiments and number of surveys taken

Year of experiment	Dimensions		Number of surveys (one per minute)
	Alongshore (m)	Cross-shore (m)	
1992	40	20	150
1994	50	20	60
1995	30	20	135
1996	30	20	71
1997	35	20	121

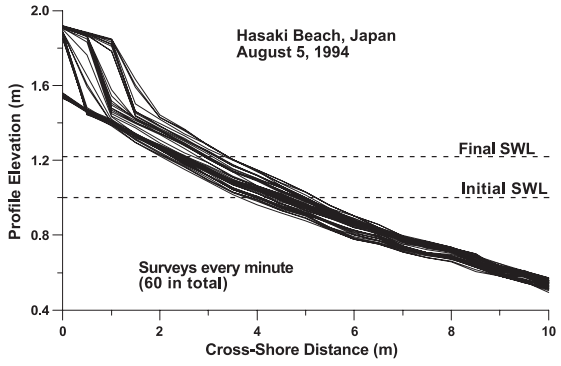

Fig. 7. Measured foreshore profiles at Hasaki Beach during the experimental run performed in 1994 (in total 60 profiles taken every minute).

4. Sediment transport formula for the swash zone

4.1. Theoretical developments

In the following, a sediment transport formula for the swash zone is developed that quantifies the net transport rate over many swash cycles. A shear-stress based bed-load transport formula is integrated over a swash cycle to yield the net transport during the cycle. The equilibrium foreshore slope is introduced into the formula so that the transport rate becomes proportional to the difference between the actual slope and its equilibrium value. Furthermore, simple parameterization of the shear stress produces a transport rate that depends on the local velocity to the power three. The local swash velocity and duration needed to calculate the transport rate is obtained by employing a ballistic model.

Madsen (1991) derived a sediment transport rate formula for the instantaneous bed load $q_b(t)$ that was further generalized in Madsen (1993) to yield,

$$\frac{q_b(t)}{\sqrt{(s-1)gd}d} = \frac{8}{1+\frac{\tan\beta(t)}{\tan\phi_m}}\left(|\psi(t)|-\psi_{cr,\beta}\right)^{3/2}\frac{\tau_b(t)}{|\tau_b(t)|} \quad (1)$$

where s is the specific weight of the sediment, g the acceleration of gravity, d the sediment diameter, β the local beach slope ($\tan\beta=dh/dx$, where h is the bottom elevation and x a cross-shore coordinate), ϕ_m the friction angle for a moving grain (about 30°), t time, and $\psi=\tau_b/(\rho_s-\rho)gd$ (Shields parameter). The subscript cr,β refers to incipient conditions for sediment movement at the slope β. Waves are assumed to propagate against the x-axis, which points offshore, and the h-axis is taken positive downwards. Thus, a beach profile with a monotonically increasing depth with distance offshore has a positive slope, which reduces the transport rate during onshore flow. At x, the transport is onshore during the uprush phase and offshore during the backwash phase.

Although Eq. (1) was derived for bedload transport under waves and currents in a homogenous fluid, it will be assumed that the general relationship is also valid in the swash when a particular location x is subject to a flow (during time periods when there is no flow, the transport is set to zero). There is an ongoing debate whether bed load or suspended load is most important in the swash zone (Horn and Mason, 1994; Hughes et al., 1997a). The ratio between these two transport modes seems to vary greatly in space and time, where marked suspended load typically is observed near the front of the uprush bore, whereas bed load prevails during other phases of the swash. Previous modeling efforts have often employed bed-load transport formulas (e.g., Hughes et al., 1997b; Masselink and Hughes, 1998), although there have been some efforts to include the suspended load (Holland et al., 1998). Shear-stress based formulas, such as Eq. (1), have previously been used to calculate the total load (i.e., bed load and suspended load together; see Van De Graaff and Van Overeem, 1979; Watanabe, 1992), so with coefficients properly tuned the model developed here should be applicable also for predicting the total load.

Integrating the transport rate over a swash cycle at x gives a mean transport $q_{b,net}$,

$$\frac{q_{b,net}}{\sqrt{(s-1)gd}d} = \frac{8I_B}{1-\frac{dh/dx}{\tan\phi_m}} - \frac{8I_U}{1+\frac{dh/dx}{\tan\phi_m}} \quad (2)$$

where,

$$I_U = \frac{1}{T}\int_{t_s}^{t_m}\left(|\psi(t)|\right)^{3/2}dt$$

$$I_B = \frac{1}{T}\int_{t_m}^{t_e}\left(|\psi(t)|\right)^{3/2}dt \quad (3)$$

in which T is the wave period, assumed to generate the swash oscillation, t_s and t_e the start and end time of the swash, respectively, at x, and t_m the time when uprush changes to backwash. Offshore transport is taken positive in Eq. (2) (in accordance with the definition of the x-axis) and the critical Shields stress was neglected in Eq. (3). If equilibrium is assumed to occur when $q_{b,net}=0$ at all points across the foreshore, Eq. (2) implies that the local equilibrium slope is $\tan\beta_e=(I_U-I_B)/(I_U+I_B)\tan\phi_m$ (Larson et al., 1999).

Reformulating Eq. (2) and using this relationship for $\tan\beta_e$ gives:

$$\frac{q_{b,net}}{\sqrt{(s-1)gdd}} = \frac{8\tan\phi_m}{\tan^2\phi_m - (dh/dx)^2}(I_U + I_B)\left(\frac{dh}{dx} - \tan\beta_e\right) \quad (4)$$

In order to compute the net transport, the time history of τ_b at x during a swash cycle must be known (τ_b appears in ψ). If the shear stress is assumed proportional to the local velocity (u) squared, the problem reduces to estimate the variation in u at x (together with an appropriate friction coefficient). Few detailed measurements of the swash velocity are available to give guidance for such an estimation (e.g., Masselink and Hughes, 1998), but data seem to indicate that the maximum onshore u occurs when the uprush bore passes a specific location and that the maximum offshore u takes place at the end of the backwash. Also, the backwash phase is longer than the uprush phase (i.e., no symmetry between the uprush and backwash phase). Water level measurements in the swash have demonstrated this asymmetry as well (Waddell, 1973a).

To proceed with the present derivation, a schematization of $u(t)$ across the swash zone will be introduced that exhibits the general observations made for the swash velocity, simultaneously as it allows for an analytical evaluation of the integrals in Eq. (3). It will be assumed that properly scaled, the velocity variation in time is approximately similar across the swash zone, that is, $u/u_o = \Gamma\{(t-t_s)/t_o\}$, where u_o and t_o is a scaling velocity and time, respectively, and Γ a function that characterizes the non-dimensional velocity variation in time at all locations in the swash zone. Here, u_o is taken as the bore front velocity and t_o as the duration of the swash at the particular location ($=t_e-t_s$). These scaling variables are calculated by considering the bore as a slug of water moving up and down the foreshore yielding (compare Shen and Meyer, 1963; Waddell, 1973a; Hughes, 1992),

$$u_o = \sqrt{u_s^2 - 2gz}$$
$$t_o = T\sqrt{1 - \frac{2gz}{u_s^2}} \quad (5)$$

where u_s is the velocity at the start of the swash ($x=x_s$) and z the elevation above the location where $x=x_s$ (z is pointing upwards). For a plane foreshore with slope $\tan\beta_{fs}$, the relationship between the elevation and the cross-shore coordinate is given by $z=(x_s-x)\tan\beta_{fs}$. The runup limit R is given by $u_0=0$, that is, $R=u_s^2/2g$. Thus, R as given by existing runup prediction formulas may be used in Eq. (5) instead of u_s, which is more difficult to obtain predictive expressions for.

Developing Eq. (4) by solving the integrals in Eq. (3) using the self-similar velocity variation (employing a quadratic dependence of τ_b on u, that is, $\tau_b=1/2f\rho u^2$) yields,

$$q_{b,net} = K_c\frac{\tan\phi_m}{\tan^2\phi_m - (dh/dx)^2}\frac{u_o^3}{g}\left(\frac{dh}{dx} - \tan\beta_e\right)\frac{t_o}{T} \quad (6)$$

where,

$$K_c = 2\sqrt{2}\frac{f^{3/2}}{s-1}\int_0^1 |\Gamma(\xi)|^3 d\xi \quad (7)$$

in which f is a friction factor and ξ a dummy integration variable. By introducing K_c, the unknown quantities f and Γ may be lumped into one non-dimensional transport coefficients with a value that essentially has to be determined through calibration against field data. Utilizing Eq. (5) and the aforementioned relationship between R and u_s in Eq. (6) gives:

$$q_{b,net} = K_c 2\sqrt{2g}R^{3/2}\left(1 - \frac{z}{R}\right)^2 \times \frac{\tan\phi_m}{\tan^2\phi_m - (dh/dx)^2}\left(\frac{dh}{dx} - \tan\beta_e\right) \quad (8)$$

Thus, to calculate the transport rate distribution in the swash zone the local slope and its equilibrium value, the elevation, and the runup height is needed, besides the values on the coefficients K_c and ϕ_m.

4.2. Comparison between transport formula and field data

Marked simplifications had to be introduced regarding the swash zone flow in order to arrive at an analytical expression for the net sediment transport

rate (Eqs. (6) and (8)). Interaction between consecutive waves in the swash zone is typically important depending on the incoming wave period in relation to the natural period of the swash oscillation (Sonu et al., 1974), which in turn is highly dependent on the foreshore slope with a more pronounced interaction for mild slopes. Furthermore, randomness of the incoming waves tends to complicate the swash interaction, although attempts have been made to model this (Mase, 1988). Finally, infiltration effects were not accounted for in the derivation, implying that the formula is only potentially meaningful for fine-grained sand where such effects are less pronounced (Masselink and Li, 2001).

Because of the simplifications introduced, the ability of the derived formula to describe swash sediment transport has to be assessed by comparison with data. As a first step to assess the applicability of the derived transport formula, the transport rate at the seaward end of the swash zone was computed using Eq. (8) and then compared with the net transport rates presented by Kubota et al. (1999); Table 1. At this location, z=0 and the transport rate is only a function of runup height and the local beach slope and its equilibrium value. Thus, Eq. (8) will reduce to:

$$q_{b,net} = K_c 2\sqrt{2g}R^{3/2} \times \frac{\tan\phi_m}{\tan^2\phi_m - (dh/dx)^2}\left(\frac{dh}{dx} - \tan\beta_e\right) \quad (9)$$

The quantities $dh/dx=\tan\beta$ and $\tan\beta_e$ were taken from Table 1, whereas the runup height was computed using the iterative formula recommended by Mayer and Kriebel (1994), where a composite slope for the swash and surf zone is used. The significant wave height was employed in calculating R. Fig. 8 illustrates the relationship between the measured sediment transport rate and a transport parameter, which is the right-hand side of Eq. (9), except the factor $K_c 2\sqrt{2}$. A reasonable correlation is obtained in the figure (explained variation is about 70%), if one run from 1994 is ignored (HA94). In this run, as pointed out previously, material added on the foreshore was shaped into a dune-like feature with an extreme beach face slope. It is expected that the transport at the toe of this dune occurred more in line with the impact theory (Fisher et al., 1986), which is not described by the present formula. The least-squares fitted straight line indicates that the derived formula has potential for computing the sediment transport in the swash zone. An optimum value on the coefficient K_c of 3×10^{-3} was obtained.

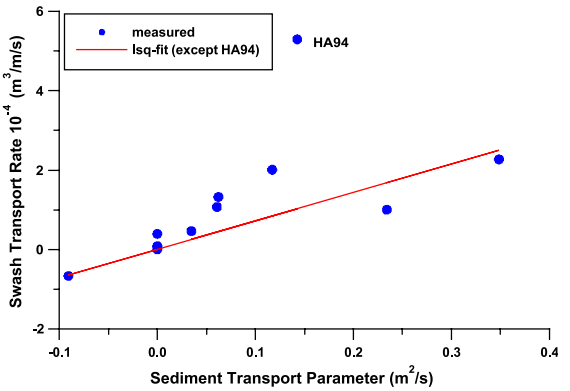

Fig. 8. Relationship between measured sediment transport rate at the seaward end of the swash zone and a transport parameter (data from Hasaki Beach, Japan).

5. Simple analytical model of foreshore response

In order to investigate the properties of the derived swash-zone transport formula and its implication for the foreshore response, a simple analytical solution was developed. The foreshore is assumed to be plane-sloping at all times from the runup limit to the still-water level, which constitutes the seaward boundary of the swash zone. Transport in or out through the seaward boundary yields an instantaneous response in the foreshore, causing a uniform adjustment of the slope. The seaward boundary remains fixed in space, implying a foreshore that rotates around the still-water line. Although such a model of the foreshore response is highly schematized, plane-sloping foreshores are typically observed in the field, if the sediment is not too coarse. Also, the shoreline often functions as conveyor of sediment (in the cross-shore direction) and remains more or less fixed in space. Thus, it is hypothesized that the simple analytical model may provide an approximate, but realistic estimate of the typical response time scale of the

foreshore to sediment exchange between the swash and surf zone.

Assuming that the transport rate at the seaward end of the swash zone can be described by Eq. (9), the change in the foreshore sand volume V_f is given by:

$$\frac{dV_f}{dt} = -q_{b,net} \tag{10}$$

As described above, the response of the foreshore was schematized to determine V_f so that an analytical solution was possible. If the foreshore evolves with an approximately constant slope $\tan\beta_f$, the foreshore sand volume exposed to transport, having a triangular shape, may be expressed as,

$$V_f = \frac{1}{2}x_s^2\beta_f \tag{11}$$

where x_s is the horizontal swash excursion, given by R/β_F for a constant foreshore slope, and small slopes were assumed (an assumption that will be made throughout this derivation). Previously, the runup prediction formula by Mayer and Kriebel (1994) was applied, but to arrive at an analytical solution the classical Hunt (1959) formula was used for which:

$$R = \beta_f\sqrt{H_oL_o} \tag{12}$$

Substituting Eq. (12) into Eq. (11), using the relationship between x_s and R, yields:

$$V_f = \frac{1}{2}H_oL_o\beta_f \tag{13}$$

Finally, Eqs. (9) and (10) are combined, simultaneously as the expressions for R and V_f from Eqs. (12) and (13), respectively, are utilized. After these manipulations, the following equation is obtained for the response of the foreshore in terms of β_f,

$$\frac{d\beta_f}{dt} = -K_c\frac{4\sqrt{2g}}{\tan\phi_m}(H_oL_o)^{-1/4}\beta_f^{3/2}(\beta_f-\beta_e) \tag{14}$$

where $(dh/dx)^2$ in the denominator of Eq. (9) was neglected (small slopes).

Eq. (14) is a nonlinear separable differential equation for which an implicit solution in β_f can be found using the initial condition that $\beta_f=\beta_{fo}$ when $t=0$. In order to generalize the solution, the following non-dimensional quantities (denoted by a prime) are introduced: $\beta'_f=\beta_f/\beta_e$, $\beta'_{fo}=\beta_{fo}/\beta_e$, and $t'=t/T$. With these quantities, the solution becomes,

$$\ln\left\{\frac{\left(\sqrt{\beta_{fo}'}-1\right)\left(\sqrt{\beta_f'}+1\right)}{\left(\sqrt{\beta_{fo}'}+1\right)\left(\sqrt{\beta_f'}-1\right)}\right\} + 2\left(\frac{1}{\sqrt{\beta_{fo}'}}-\frac{1}{\sqrt{\beta_f'}}\right) = K_c'\,t' \tag{15}$$

where:

$$K_c' = K_c\frac{8\sqrt{\pi}}{\tan\phi_m}\left(\frac{H_o}{L_o}\right)^{-1/4}\beta_e^{3/2} \tag{16}$$

Fig. 9 plots the solution given by Eq. (15) for various values on β'_{fo}, both for cases when the foreshore erodes and accretes. Thus, the analytical solution is valid for either case, and the direction of transport is determined by the deviation from β_e. An initial profile with $\beta_{fo}>\beta_e$ yields erosion, whereas the opposite condition produces accretion. The magnitude of the response is given by K'_c.

Starting from a given initial slope β'_{fo}, the slopeβ'_f is reached after a certain value on $K'_c\,t'$ is attained in accordance with the non-dimensional solution in Eq. (15). Thus, it is possible to compare the foreshore response in dimensional terms for different cases, quantifying the influence of the wave parameters, if the response for a particular $K'_c\,t'$-value is investigated. Two cases (index 1 and 2) where $(K'_c\,t')_1=(K'_c\,t')_2$, implies the same value on β'_f. Assuming that β_e is constant but the waves are

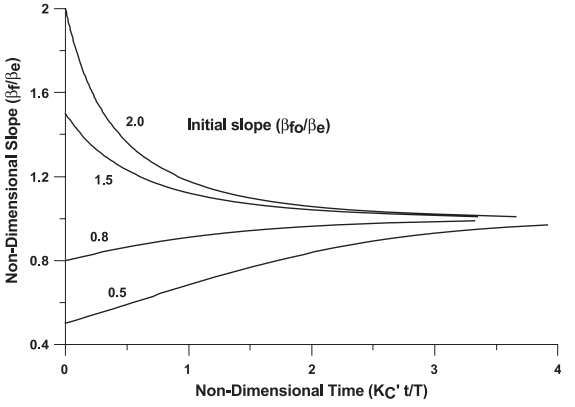

Fig. 9. Analytical solution to describe the evolution of the foreshore slope as a function of time and initial deviation from equilibrium conditions (solution expressed in non-dimensional quantities).

changing, the following relationship between the two wave conditions is obtained:

$$\frac{t_1}{t_2} = \left(\frac{H_{o1}}{H_{o2}}\right)^{1/4}\left(\frac{T_1}{T_2}\right)^{1/2} \quad (17)$$

Thus, the wave period would have a greater influence than the wave height because of the larger power. For example, doubling the wave period would imply about 40% longer time period to achieve the same slope response, whereas the same change in the wave height would only give less than a 20% increase. The reason why the time for a certain foreshore response increases with the wave height and period is because of the larger sand volume involved in the adjustment through the larger runup height. From Fig. 9 it may also be seen that for the range of β'_{fo}-values tested, near-equilibrium (the slope is within about 2% of its equilibrium value) is attained when $K'_c t'$ exceeds the value 4.0. Expressing this criterion in a different form yields,

$$\frac{t_{eq}}{T} = \frac{1}{2K_c}\frac{\tan\phi_m}{\sqrt{\pi}}\left(\frac{H_o}{L_o}\right)^{1/4}\frac{1}{\beta_e^{3/2}} \quad (18)$$

where t_{eq} is the time when near-equilibrium is achieved. For typical values on the quantities in Eq. (18), it will take 200–400 wave periods to reach equilibrium.

6. Numerical model of foreshore evolution

6.1. Model formulation

In order to further evaluate the derived formula for computing swash-zone sediment transport rates, Eq. (8) was utilized in a numerical model to predict the evolution of the foreshore for the experimental runs from Hasaki Beach. Only runs where sand was added on the foreshore was used (that is, erosive cases) and the previously discussed run HA94 was excluded because of its unusual geometry. This left four runs to be simulated, for which 60 to 150 surveyed profiles were available from each run. In the simulations, a limited number of surveys were used for comparison, selected to cover the evolution of the foreshore in a representative manner. Only the profile evolution in the swash zone was modeled (i.e., from the runup limit to the still-water level) which made it difficult to formulate an appropriate boundary condition at the seaward end of the grid. At the shoreward end the grid extended beyond the runup height, where the transport rate becomes zero. The condition at the seaward boundary was no change in bottom elevation implying that sediment could freely be transported out from the grid. In three of the four runs modeled, such a simple seaward boundary condition seemed acceptable, but in one run (HA92) the profile retreated markedly around the still-water level and the model failed to capture this response.

Time series of water level elevation measured some distance seaward of the swash zone (in water depths between 0.5 and 1.0 m) were used to derive the wave input to the model. The statistical wave properties (energy-based significant wave height H_{mo} and significant wave period T_s) were computed based on 10 min time periods together with the mean water level (changing during a run because of the rising tide). Input waves and water level were given by the computed time series of the statistical values. This was preferred to, for example, employing individual waves identified in the water level time series, since it is expected that Eq. (8) would describe the transport rate in an average sense and not for a single runup event. The still-water level, which varied in time according to the tide, determined the start of the swash zone.

The numerical model calculations involved the following main routines at every time step: (1) input wave properties and mean water elevation; (2) runup height using the iterative method proposed by Mayer and Kriebel (1994); (3) swash-zone sediment transport across the foreshore using Eq. (8); and (4) sediment volume conservation equation to update the foreshore profile. The equilibrium slope was specified based on the field measurements by Kubota et al. (1999) and $\tan\phi_m$=30°, so the only parameter to fit was K_c. Instead of selecting some runs for calibrations and others for validation, the value of K_c was optimized individually for all four runs using a least-square error. This was done mainly to establish a range of values on K_c that might be reasonable to utilize in field applications. The transport coefficient K_c is expected to depend on various factors, where the grain size should be the leading one because of the friction factor (see Eq. (7)). In the present study

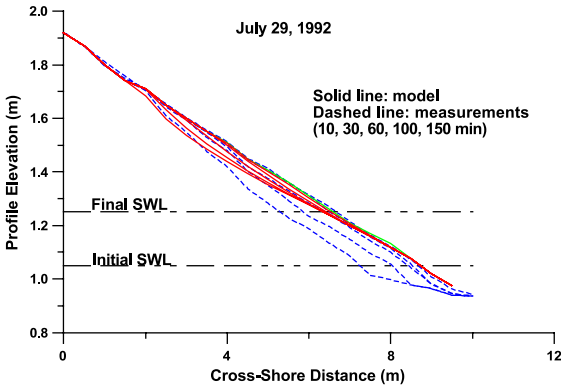

Fig. 10. Comparison between measured and calculated profile response in the swash zone for Run HA92.

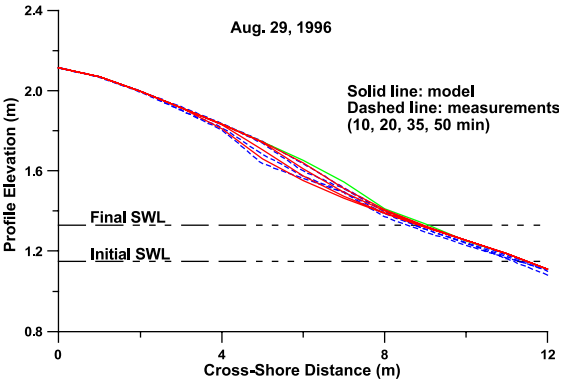

Fig. 12. Comparison between measured and calculated profile response in the swash zone for Run HA96.

basically only one sand size was investigated, implying that if the present formula is used for widely different grain sizes, care should be taken in selecting the K_c-value.

Figs. 10–13 display the results of the simulations with the model compared to the measurements for Runs HA92, HA95, HA96, and HA97, respectively. Five measured foreshore profiles, selected from the large number of surveys made during a run, are shown for each run (survey times from the start of the run, as well as the run date, are given in the figures). The local coordinate system defined by Kubota et al. (1999) for the measurements are used in the figures. Mean water levels at the beginning and end of the run are also plotted to illustrate the tidal variation. In the following, a brief discussion of the model results for each run is given together with the prevailing forcing conditions. The wave heights and periods given below differs a bit from the values presented in Table 1 since these values encompass slightly different measurement periods.

6.2. Run HA92

During this run the still-water shoreline retreated significantly, and, as previously mentioned, the simple boundary condition at the seaward end of the swash zone constituted a poor description of the profile evolution here. Nevertheless, the profile response in the upper part of the swash zone was reasonably well reproduced by the model, including the runup height (Fig. 10). The mean H_{mo} was approximately 0.40 m during the run and mean T_s=13.0 s, whereas the tide rose from 1.05 to 1.25 m (in the local reference system). The optimum K_c-value was 1×10^{-3}.

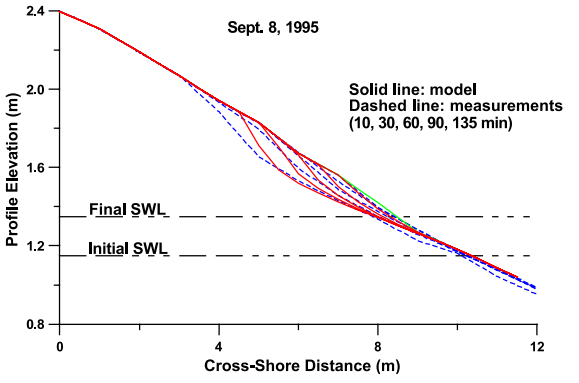

Fig. 11. Comparison between measured and calculated profile response in the swash zone for Run HA95.

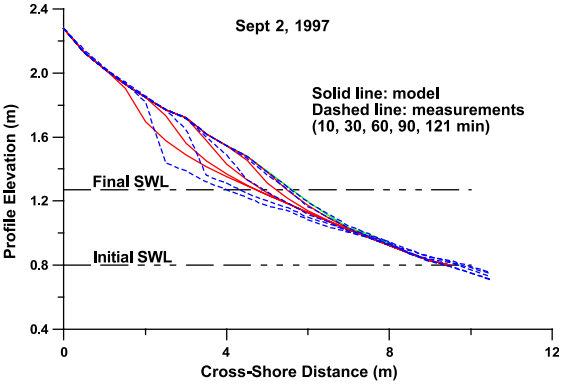

Fig. 13. Comparison between measured and calculated profile response in the swash zone for Run HA97.

6.3. Run HA95

In this run, the mean H_{mo} and T_s were 0.50 m and 8.2 s, respectively. The tide increased the mean water level from 1.15 to 1.35 m during the measurements. As opposed to Run HA92, the seaward boundary condition works well, whereas the runup height is somewhat underpredicted Fig. 11. Overall, the profile response is satisfactorily simulated, although the model tends to produce a steeper profile shape near the runup limit. A value of K_c=2.1×10^{-3} gave the best fit to the data.

6.4. Run HA96

In all runs the entire measurement period was employed in the comparison with the model simulation results. However, for Run HA96, the final 20 min (out of 71 min) were not included because the erosion substantially increased during this period, although the wave conditions remained about the same as in the beginning of the period. The explanation for the increase in erosion is not known, but the response was not judged representative for testing the present model. Possibly, some long wave activity was present during the final phase of the measurements that could enhance the sediment transport. For the time period shown in Fig. 12 the agreement is excellent across most of the foreshore, including the runup height. The optimum K_c-value was determined to be 2.3×10^{-3} based on the first part of the measured profile time series (by increasing this value to about 4.5×10^{-3} the erosion after 71 min could be well predicted, albeit at the expense of the agreement for the profiles during the main portion of the run). The mean H_{mo} was 0.55 m and the mean T_s=14 s, whereas the tide rose from 1.15 to 1.35 m (during the simulation period).

6.5. Run HA97

During this run the mean H_{mo} and T_s were 0.55 m and 13 s, respectively, and the mean water elevation varied from 0.80 to 1.35 m. The agreement between calculations and measurements are satisfactory Fig. 13, except close to the runup limit where the predicted shape is too steep and the erosion too large (compare Run HA95). Thus, the shape and retreat of the scarp that forms at the shoreward limit because of the erosion is not well described. It is expected that once a scarp forms with its steep slope, transport due to wave impact will be important and the present transport formula is not appropriate (e.g., Nishi and Kraus, 1996). The optimum K_c-value was 1.2×10^{-3}.

7. Discussion

The model developed to compute the net sediment transport in the swash zone involved a number of simplifications in order to arrive at a robust formulation that yields realistic and stable predictions of the foreshore evolution. A more detailed model aiming at resolving the variation in the transport rate during a swash cycle, and not the net transport over many cycles like the present model does, would be quite sensitive to small errors in the transport predictions that would grow to finally produce unrealistic foreshore responses. The major assumptions behind the swash sediment transport model are: (1) the total transport rate is proportional to the local, instantaneous shear stress; (2) the velocity and duration of the leading edge of the swash can be described by ballistic theory; (3) the local velocity of the swash at any given location is self-similar when scaled with the leading edge velocity and duration; and (4) the equilibrium slope of the foreshore may be specified together with some other coefficient values such as the transport rate coefficient (K_c) and the friction angle. When implementing the model to simulate the foreshore evolution further assumptions were made, including using the runup height to determine the initial speed of the uprushing wave and employing a boundary condition that implied no change in elevation at the mean water level (zero gradient in the transport rate).

In the validation of the transport formula towards the net transport rate at the shoreline obtained in the field experiments, only a limited range of grain sizes was covered. Thus, it remains to be shown that the transport formula can work for other grain sizes as well, especially for coarser sizes where infiltration effects become important. It is questionable whether the self-similarity assumption would be relevant on a beach where infiltration is large, preventing significant backwash along portions of the foreshore.

Another limitation of the model encountered in the validation is the steepness of the foreshore. The model is only applicable for slopes small enough to ensure that shear stress from the flowing water is the main mechanism of sediment transport. For really steep slopes, for example, what occurs along the face of a dune, other transport mechanisms would dominate such as wave impact.

The parameterization of the leading edge velocity and duration using ballistic theory have been shown to yield satisfactory results in several previous studies (Hughes, 1992; Hughes, 1995; Puleo and Holland, 2001), although friction losses should be taken into account to yield close agreement with measurements. In the present model, friction is not included directly in the velocity calculations, but only indirectly through the calibration of K_c. However, to modify the computations of u_o and t_o in order to include friction would be straightforward.

To apply the model a number of coefficients must be assigned proper values. The most difficult one to determine is K_c and the present study showed quite some variation in the optimum value of this coefficient for the various experimental cases, indicating that K_c would depend on some additional physical factors. As previously pointed out, K_c should depend on the grain size, although the present data set does not allow for a quantification of this dependence. Another factor that should be important in this respect, not explicitly taken into account in the modeling, is wave–wave interaction in the swash (Kubota et al., 1993; Baldock and Holmes, 1997, 1999). Depending on the incoming wave properties and the foreshore slope, consecutive waves may interact because of catch-up and absorption, leading to a period for the characteristic swash cycle that is different from the incoming wave period.

In order to investigate the influence of wave–wave interaction in the swash on the transport rate coefficient, the optimal K_c-values were correlated with the ratio between the wave period (T_s) and the swash period (T_{sw}), where the latter was taken from the measurements by Kubota et al. (1999). The swash period was derived based on the oscillations measured by the swash gage after conversion to vertical distance. This analysis showed a tendency of decreasing K_c with increasing T_s/T_{sw}, although the number of data points is quite limited (in total only four cases). More data are needed to establish a predictive relationship between K_c and T_s/T_{sw}. Mase and Iwagaki (1984) studied the relationship between the normalized period of the swash oscillation and the surf similarity parameter. Thus, it may be possible to predict T_s/T_{sw} based on the incoming wave properties.

8. Conclusions

A unique set of field measurements were employed to investigate swash-zone sediment transport and foreshore evolution. By artificially modifying the foreshore slope, significant net transport in the swash could be observed and the analysis yielded information on the main physical quantities governing the net transport and the associated foreshore response. In total six experiments were carried out, in most cases also including measurements for the natural beach slope, before modification. The emphasis was on making the foreshore steeper implying offshore sediment transport and erosion. All cases showed a foreshore profile that evolved back to its equilibrium value prior to the slope modification. In most cases this response implied little change at the seaward boundary of the swash, that is, this point mainly conveyed the material towards the offshore (for the case of erosion).

The formula developed to calculate the net sediment transport in the swash zone showed good agreement with the transport rate measurements at the seaward end of the swash. Furthermore, the simulations of the distribution of the transport across the swash zone yielded encouraging agreement with measurements when the time evolution of the foreshore profile was modeled under the action of waves and rising mean water level. The average value on the transport coefficient (K_c) for the four experimental runs modeled was 1.6×10^{-3}, which is judged to be a representative value for beaches consisting of fine sand. Analysis of a limited number of cases indicated that K_c might be dependent upon the relationship between the incident wave period and the swash period, which quantifies wave–wave interaction in the swash.

However, several improvements are needed before a general, robust, and reliable mathematical

model of the swash zone transport is obtained. A limitation in the present model was that only the evolution on the foreshore was described and there was no coupling to the rest of the profile (i.e., only a simple boundary condition on the seaward side). In reality, there is a strong interaction between the surf zone and swash zone that needs to be properly described. Thus, the next step is to couple the present swash zone model to a model for the evolution of the rest of the profile.

Acknowledgements

The support of the Swedish Natural Science Research Council (NFR) is gratefully acknowledged. This work was also partly funded by the project "Study on erosion control of national land", through the Interdisciplinary Global Joint Research Grant for Nihon University in 2001, and the Inlet Modeling System Work Unit of the Coastal Inlets Research Program, U.S. Army Corps of Engineers. The paper benefited greatly by the insightful reviews by Drs. Tony Butt and Tom Baldock.

References

Baldock, T.E., Holmes, P., 1997. Swash hydrodynamics on a steep beach. Proceedings Coastal Dynamics '97, ASCE, pp. 784–793.

Baldock, T.E., Holmes, P., 1999. Simulation and prediction of swash oscillations on a steep beach. Coastal Engineering 36, 219–242.

Butt, T., Russell, P., 1999. Suspended sediment transport mechanisms in high-energy swash. Marine Geology 161, 361–375.

Elfrink, B., Baldock, T., 2002. Hydrodynamics and sediment transport in the swash zone: a review and perspectives. Coastal Engineering 45, 149–167.

Fisher, J.S., Overton, M.F., Chisholm, T., 1986. Field Measurements of dune erosion. Proceedings of the 20th Coastal Engineering Conference, ASCE, pp. 1107–1115.

Holland, K.T., Puleo, J.A., 2001. Variable swash motions associated with foreshore profile change. Journal of Geophysical Research 196 (C3), 4613–4623.

Holland, K.T., Sallenger, A.H., Raubenheimer, B., Elgar, S., 1998. Swash zone morphodynamics and sediment transport processes. Proceedings of the 26th Coastal Engineering Conference, ASCE, pp. 2799–2811.

Horn, D., Mason, T., 1994. Swash zone transport modes. Marine Geology 120, 309–325.

Hotta, S., Mizuguchi, M., 1980. A field study of waves in the surf zone. Coastal Engineering in Japan 23, 59–79.

Hughes, M.G., 1992. Application of a non-linear shallow water theory to swash following bore collapse on a sandy beach. Journal of Coastal Research 8 (3), 562–578.

Hughes, M.G., 1995. Friction factors for wave uprush. Journal of Coastal Research 13, 1089–1098.

Hughes, M.G., Masselink, G., Brander, R.W., 1997a. Flow velocity and sediment transport in the swash zone of a steep beach. Marine Geology 138, 91–103.

Hughes, M.G., Masselink, G., Hanslow, D., Mitchell, D., 1997b. Toward a better understanding of swash zone sediment transport. Proceedings of Coastal Dynamics '97, ASCE, pp. 804–813.

Hunt, I.A., 1959. Design of seawalls and breakwaters. Journal of the Waterways and Harbors Division 85 (3), 123–152.

Katori, S., Tanaka, K., Kubota, S., Takezawa, M., 2001. Field measurements of on–offshore sediment transport rate in the swash zone. Proceedings of Coastal Dynamics '01, ASCE, pp. 898–907.

Kriebel, D.L., 1994. Swash zone wave characteristics from SUPERTANK. Proceedings of the 24th Coastal Engineering Conference, ASCE, pp. 2207–2221.

Kriebel, D.L., Dean, R.G., 1985. Numerical simulation of time-dependent beach and dune erosion. Coastal Engineering 9, 221–245.

Kubota, S., Mizuguchi, M., Takezawa, M., 1993. Prediction of field swash and reflected wave distributions. Coastal Engineering in Japan 36 (2), 111–131.

Kubota, S., Hida, Y., Takezawa, M., 1994. Two dimensional change of swash slope. Proceedings of the International Conference on Hydro-Technical Engineering for Port and Harbor Construction, Yokosuka, Japan, pp. 1193–1209.

Kubota, S., Naito, A., Matsumura, T., Takezawa, M., 1997. Field observations of topography change on an artificial beach face due to on–offshore transport. Proceedings of Combined Australasian Coastal Engineering and Ports Conference, Christchurch, New Zealand, pp. 325–330.

Kubota, S., Katori, S., Takezawa, M., 1999. Relationship between on–offshore sediment transport rate on the beach face and wave energy. Proceedings of Coastal Sediments '99, ASCE, pp. 447–462.

Larson, M., Kraus, N.C., 1989. SBEACH: Numerical model for simulating storm-induced beach change. Report 1: Empirical foundation and model development. Technical Report CERC-89-9, USAEWES, Vicksburg, MS.

Larson, M., Kraus, N.C., Wise, R.A., 1999. Equilibrium beach profiles under breaking and non-breaking waves. Coastal Engineering 36, 59–85.

Longo, S., Petti, M., Losada, I.J., 2002. Turbulence in the swash and surf zones: a review. Coastal Engineering 45, 129–147.

Madsen, O.S., 1991. Mechanics of cohesionless sediment transport in coastal waters. Proceedings of Coastal Sediments '91, ASCE, pp. 15–27.

Madsen, O.S., 1993. Sediment transport on the shelf. Proceedings of the Sediment Transport Workshop DRP TA1, 8–9 June. CERC, Vicksburg, MS.

Mase, H., 1988. Spectral characteristics of random wave run-up. Coastal Engineering 12, 175–189.

Mase, H., Iwagaki, Y., 1984. Run-up of random waves on gentle slopes. Proceedings of the 19th Coastal Engineering Conference, ASCE, pp. 593–609.

Masselink, G., Hughes, M., 1998. Field investigation of sediment transport in the swash zone. Continental Shelf Research 18, 1179–1199.

Masselink, G., Li, L., 2001. The role of swash infiltration in determining the beachface gradient: a numerical study. Marine Geology 176, 139–156.

Mayer, R.H., Kriebel, D.L., 1994. Wave runup on composite-slope and concave beaches. Proceedings of the 24th Coastal Engineering Conference, ASCE, pp. 2325–2339.

Miller, R.L., 1968. Experimental determination of run-up of undular and fully developed bores. Journal of Geophysical Research 73 (14), 4497–4510.

Nishi, R., Kraus, N.C., 1996. Mechanism and calculation of sand dune erosion by storms. Proceedings of the 25th Coastal Engineering Conference, ASCE, pp. 3034–3047.

Puleo, J.A., Holland, K.T., 2001. Estimating swash zone friction coefficients on a sandy beach. Coastal Engineering 43, 25–40.

Puleo, J.A., Beach, R.A., Holman, R.A., Allen, J.S., 2000. Swash zone sediment suspension and transport and the importance of bore-generated turbulence. Journal of Geophysical Research 105 (C7), 17021–17044.

Richmond, B.M., Sallenger, A.H., 1984. Cross-shore transport of bimodal sands. Proceedings of the 19th Coastal Engineering Conference, ASCE, pp. 1997–2008.

Roelvink, J.A., Brøker, I., 1993. Cross-shore profile models. Coastal Engineering 21, 163–191.

Sallenger, A.H., Richmond, B.M., 1984. High-frequency sediment oscillations in the swash zone. Marine Geology 60, 155–164.

Shen, M.C., Meyer, R.E., 1963. Climb of a bore on a beach: Part 3. Run-up. Journal of Fluid Mechanics 16, 113–125.

Sonu, C., Pettigrew, N., Fredericks, R.G., 1974. Measurement of swash profile and orbital motion on the beach. Proceedings of Ocean Wave Measurement and Analysis, ASCE, pp. 621–638.

Sunamura, T., 1984. Onshore–offshore sediment transport rate in the swash zone of laboratory beaches. Coastal Engineering in Japan 27, 205–212.

Van De Graaff, J., Van Overeem, J., 1979. Evaluation of sediment transport formulae in coastal engineering practice. Coastal Engineering 3, 1–32.

Waddell, E., 1973a. Dynamics of swash and implication to beach response. Technical Report vol. 139. Coastal Studies Institute, Louisiana State University, Baton Rouge, LA.

Waddell, E., 1973b. A field investigation of swash characteristics. Coastal Engineering in Japan 16, 61–71.

Watanabe, A., 1992. Total rate and distribution of longshore sand transport. Proceedings of the 23rd Coastal Engineering Conference, ASCE, pp. 2528–2541.